Report Title: **"Six Month Technical Progress Report for the Airborne, Optical Remote Sensing of Methane and Ethane for Natural Gas Pipeline Leak Detection"**

Type of Report: Semi-Annual

Reporting Period Start Date: October 14, 2003

Reporting Period End Date: April 13, 2004

Principal Author: Mr. Jerry Myers

Date Report Was Issued: May 12, 2004

DOE Award Number: DE-FC26-02NT41632

Name and Address of Submitting Organization:
Ophir Corporation
10184 W. Belleview Ave., Suite 200
Littleton, CO 80127

Disclaimer

Abstract

Ophir Corporation was awarded a contract by the U. S. Department of Energy, National Energy Technology Laboratory under the Project Title “Airborne, Optical Remote Sensing of Methane and Ethane for Natural Gas Pipeline Leak Detection” on October 14, 2002. The third six-month technical report contains a summary of the progress made towards finalizing the design and assembling the airborne, remote methane and ethane sensor. The vendor has been chosen and is on contract to develop the light source with the appropriate linewidth and spectral shape to best utilize the Ophir gas correlation software. Ophir has expanded upon the target reflectance testing begun in the previous performance period by replacing the experimental receiving optics with the proposed airborne large aperture telescope, which is theoretically capable of capturing many times more signal return. The data gathered from these tests has shown the importance of optimizing the fiber optic receiving fiber to the receiving optic and has helped Ophir to optimize the design of the gas cells and narrowband optical filters. Finally, Ophir will discuss remaining project issues that may impact the success of the project.

Table of Contents

List of Figures

List of Tables

1 Experimental

1.1 Exploring Near Infrared (IR) Light Transmission Through Methane Gas Cells

A problem with etalon shifts in the gas cells was seen during previous tunable Agilent Model 81640A laser scans of the methane absorption line at 1640.38 nm. Very different behavior was noticed during scans of the Triad Technology fabricated (7 cm or 2.75 inches internal pathlength) methane cell with Brewster angle windows, and the Ophir fabricated gas cell pair (25.4 cm or 10 inches internal pathlength) with normal angle windows reused from a previous DOE pulsed lidar project. The Ophir gas cells have had their windows replaced for the airborne DOE project; they now use plane parallel sapphire windows normal to the light beam axis passing through the cell. The gas cell etalon drifts in the Ophir gas cells, as observed across the methane spectral lines are sufficient to mask, obscure, and affect the magnitude of the narrowband line fingerprint of methane.

The setup for conducting these absorption measurements was simple and is shown in Figure 1. The laser source was set to an output power of –5dBm, and can be scanned in wavelength under computer control. The laser step size for all the runs in this test was 0.001 nm, and detector dwell time was 100 μm.

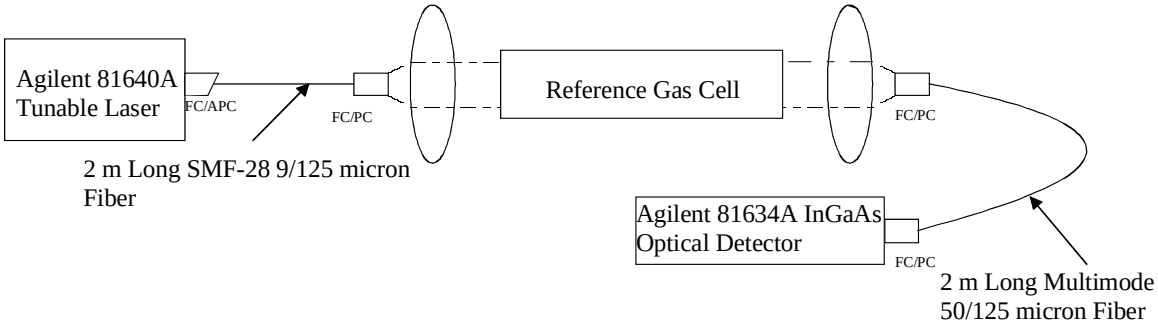

Figure 1. Optical Circuit Used to Measure Etalon Drift Through Reference Gas Cells

1.2 Short Optical Path Methane Absorption Testing Using a Narrowband Tunable Laser

This experiment is intended to replicate methane absorption measurements at an optical pathlength of 7.6 m (25 ft) one way, using the gas correlation software and a very narrowband tunable laser. The Agilent Model 81640A narrowband laser can be temperature tuned to reach 1640 nm in wavelength with a maximum output of less than 1 mW. The output power of the laser limits the experiment to very short optical pathlengths and the wavelength limits the scan to only a few methane absorption lines (ethane absorption occurs at higher wavelengths).

The design setup for this experiment is shown in Figure 2. The methane gas cell has been packaged into a metal toolbox, along with the optical splitter to allow for easy outdoor measurements.

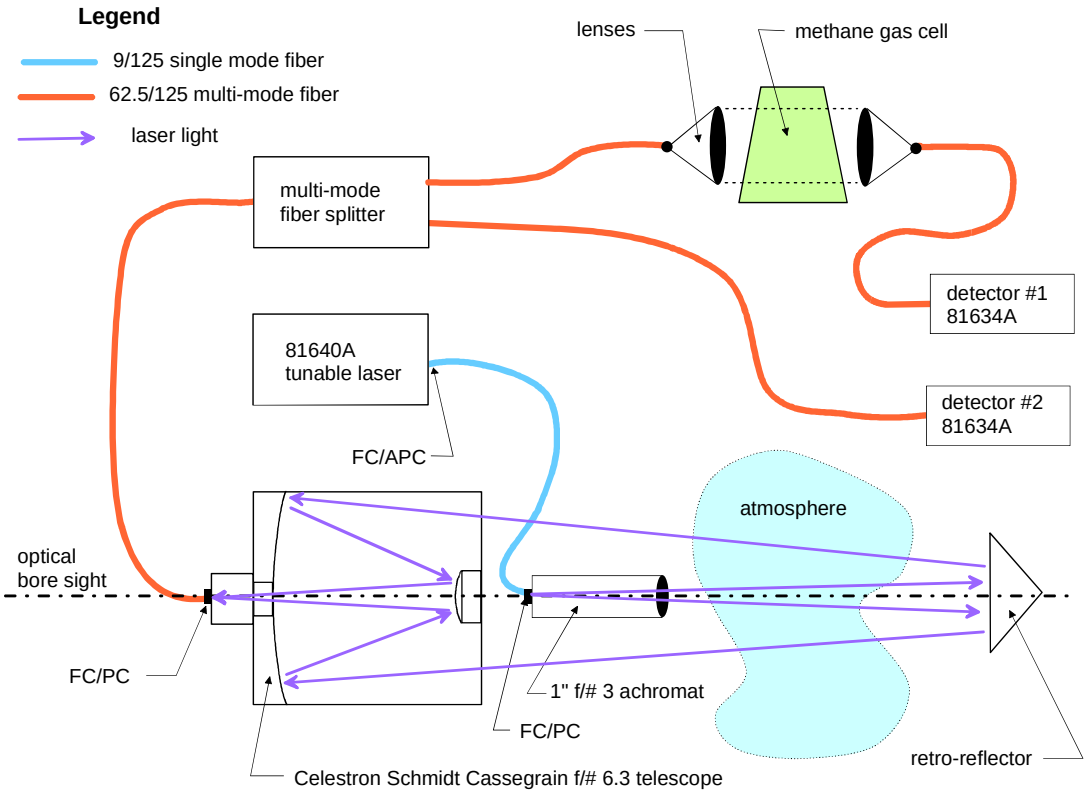

Figure 2. Experimental Setup for Short Optical Path Methane Absorption Measurements

1.3 Target Reflection Measurements at 150 m (500 ft) Optical Path Using a Co-Aligned Large Aperture 14-Inch Schmidt Cassegrain Telescope and a 1550 nm Erbium Doped Fiber Amplifier

1.3.1 Previous Target Reflectance Measurements Using a Co-Aligned 2-Inch Receiving Optic and a 1550 nm Erbium Doped Fiber Amplifier

The Second Six-Month Technical Report summarized the results of the extensive reflectance testing using the 1550 nm 1-Watt Erbium doped fiber amplifier and the small 2-inch lens tube. These results indicated the following:

- Many surfaces that will be encountered by an airborne optical system reflect light similar in nature and magnitude to a true Lambertian surface (light is reflected back in all directions). Moist surfaces tend to limit the reflected light at 1555 nm.
- It is important to have the angle of incidence from the aircraft receiver to the ground at normal or 90 degrees.
- With the 2-inch receiver and the co-aligned fiber laser, the amount of reflected light from a true Lambertian surface at 50 m produced acceptable return of 32 nW into a fairly small multimode 50 μm fiber cable.
- The use of narrowband filters will help to keep background solar noise below several tens of picowatts.
- There was significant light leakage through the fiber connectors. Serious attention needs to be placed upon limiting this leakage.
- Ophir measured surprisingly large (14.4 nW with a narrowband filter) reflected signals off of a grassy surface at a severe incidence angle at 50 m distance.
- A larger receiver optic of 14-inches aperture should theoretically yield equivalent light gathering power to the 2-inch optic at an expanded distance of 350 m.

1.3.2 Setup and Procedure for Conducting Target Reflectance Measurements with Large 14-Inch Aperture Telescope

This series of tests was performed to expand upon the earlier target reflectance measurements using a 1 Watt (W) 1550 nm fiber amplifier, 2-inch receiver optics, and a Lambertian reflector. The new setup for these tests is shown in Figure 3 and shows the addition of a large 14–inch aperture Schmidt-Cassegrain Telescope (SCT) as the signal reflection receiver. Many of the parts listed in Figure 3 were identical to those used during the previous target reflectance testing. A continuous, non-modulated current was used to drive the 1 W fiber amplifier.

The telescope was an F# 11 Schmidt-Cassegrain design, and as such includes a large primary mirror and a secondary mirror that partially obscures the incoming light. The light path enters the opening and is gathered by the primary mirror and focused onto the secondary obscuring mirror, and then refocused through an opening in the primary onto a small spot. The main advantage of this type of telescope is that the optical pathlength is considerably shortened with the folded path, and this allows for a much shorter overall length. The entire length of the 14-inch telescope is 79 cm (31 in), which allows Ophir to mount the telescope vertically within the airplane looking downward (the most efficient configuration). The focused light is gathered at the focal point of the telescope behind the rear-mounting flange onto multimode fiber; originally a fiber core size of 62.5 μm was used. As the testing progressed, larger core fiber was used as replacement receiver fiber.

The F# of the telescope can be changed to F# 2, if the secondary mirror is removed and the gathered light is allowed to focus at a spot in front of the telescope. This smaller F# in effect increases the light gathering capability, but increases the complexity of the mounting hardware for the receiver fiber. This configuration was tested thoroughly to better evaluate its performance.

An Agilent Model 8164 mainframe optical multimeter was used with either a Model 81634A optical low-noise detector or a Model 81624A large area detector. The choice of these detectors easily allowed Ophir to vary the receiver fiber core size that interfaces with the telescope. All of the reflectance testing during this performance period was done without the use of the narrowband optical filter within the Optical Spectrum Analyzer. Most of the testing was performed during the evening hours, where background solar light was not an issue. Nighttime testing was the norm due to the inability to see the invisible near-IR 1550 nm light with Ophir's existing viewing equipment during the daytime, especially at longer optical pathlengths. Ophir did receive a loaner IR viewing camera from ElectroPhysics Inc., but the combination of the inability of the camera to display IR light within solar background and the limited battery life made it useless in our test configuration. Ophir decided to use a small (2 ″ x 3 ″) IR light activated sensing card to locate the IR beam at night. As long as a visible light source was first used to locate and focus the output beam, the sensing card worked well. Ophir is hoping to obtain a larger area IR sensing card from the manufacturer to better aid in changing the focus spot size at the target.

Unless otherwise stated, the output power of the 1550 nm fiber amplifier was limited to around 500 mW.

The target reflectance tests were basically performed over a one-month period, with variations in the testing resulting from the results or lack of results. Optical noise was less of an issue during these tests, due to lack of solar background light. The optical range of the tests was set at 150 m (500 ft) one-way to simulate actual flight viewing conditions. The tests that were performed include the following:

- Using a co-aligned laser output and telescope receiver, measure the reflectance off of a Lambertian target at 150 m with standard 62.5 μm core size receiver optical fiber.

- Reconfiguring the telescope as an F# 2 telescope, using the Faststar option, measure the back reflection into the 62.5 μm fiber coupled detector.
- Vary the field of view (FOV) spot size of the large telescope at the target to determine the impact on light collection. Likewise, vary the output laser spot size at the target to determine the impact on light gathering.
- Compare the performance of the large aperture reflecting telescope to the 2-inch focusing optic (used in the previous tests).
- Determine the impact of the obscuration on the total light gathering capabilities of the large telescope by moving the light spot slightly off-center with the telescope FOV.
- Replace the low-noise small active area detectors with the large (5 mm) diameter optical detectors, remove the fiber from the telescope focusing mount, and manually focus the light in free-space onto the detector. This test will illustrate the impact of increasing the focus spot size on light gathering capabilities.
- Reconnect larger core fiber from the telescope to the large area detectors. Determine impact of using larger core fiber at the telescope focal point.

A photograph of the test setup can be seen in Figure 19.

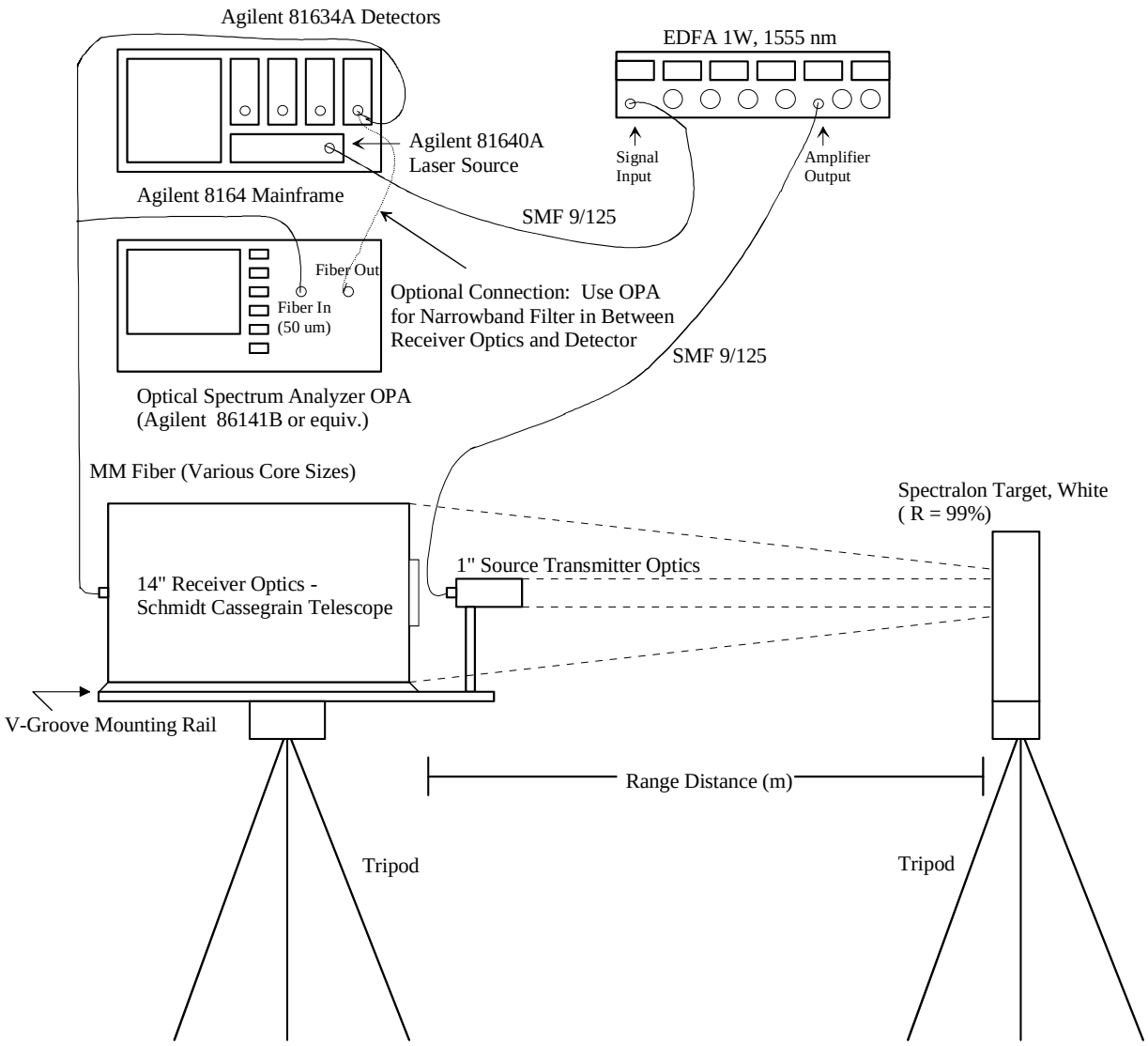

Figure 3. Setup for Target Reflectance Test Using Large 14-Inch Aperture Telescope

2 Results and Discussion

2.1 Data Results of Laboratory and Field Testing

2.1.1 Impact of Gas Cells on Optical Spectral Transmission

First the laser was scanned over a spectral range from 1639.9 to 1640.8 nm through a 25.4 cm (10 in) free air path with no cell inserted with the results shown in Figure 4. A wider scan was next performed from 1630.8 to 1640.8 nm as a second baseline, as shown in Figure 5.

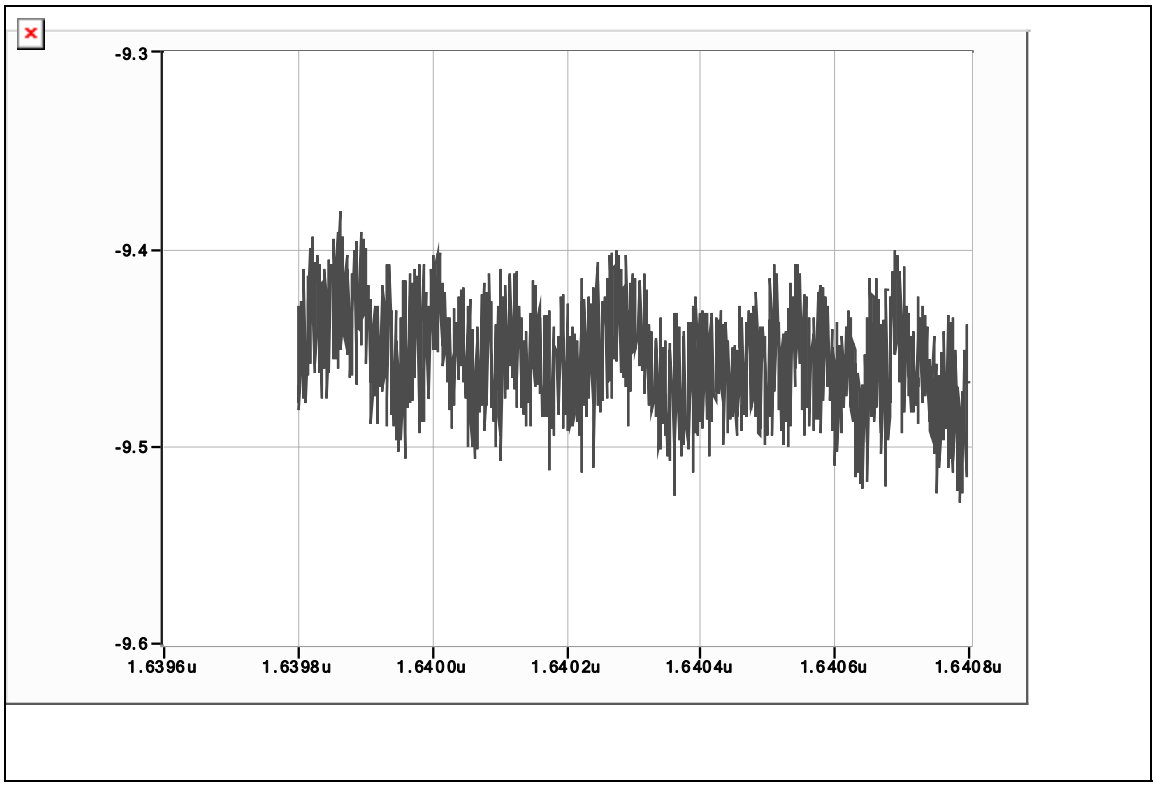

Figure 4. Baseline Scan from 1639.8 to 1640.8 nm Showing the Background Optical Noise of the System

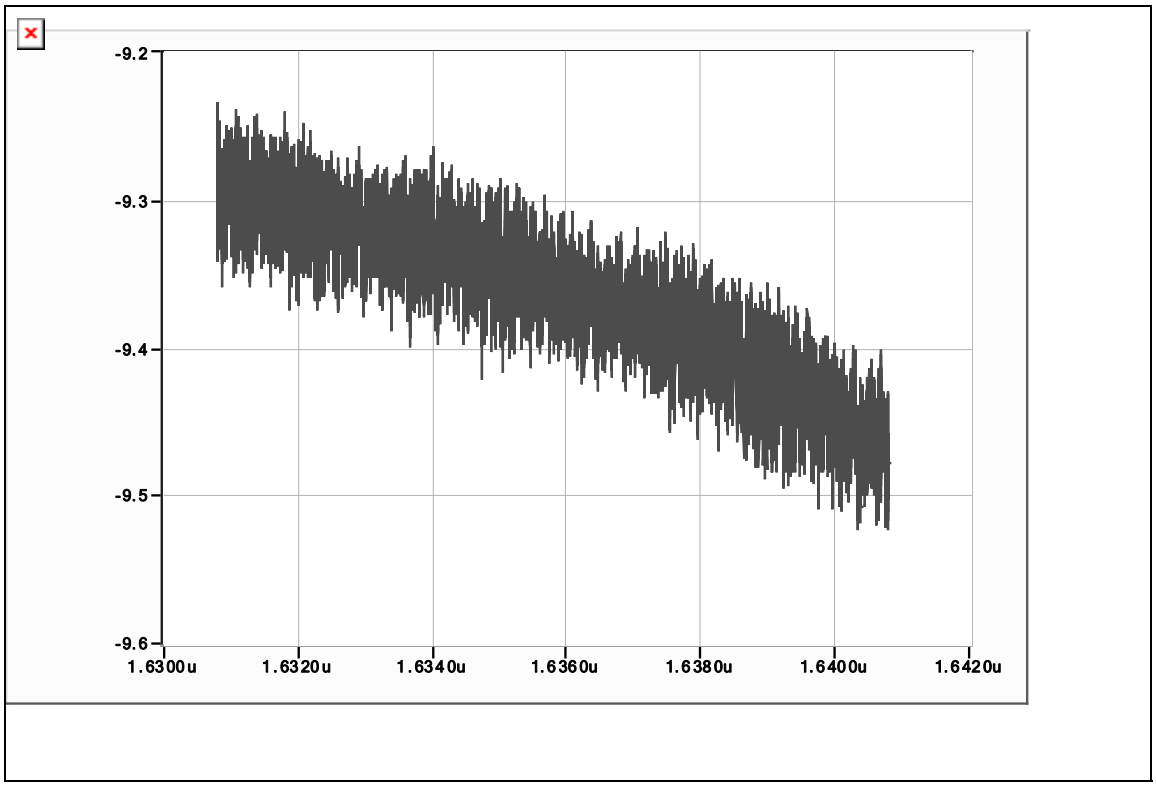

Figure 5. Baseline Scan from 1630.8 to 1640.8 nm Showing the Background Optical Noise of the System

The baseline scans of room air were stable over wavelength on 1 nm and 10 nm scales, and the autoranging graphs showed a root-mean-square (rms) noise level of about 0.04 dB (about 1%).

The two scans were now repeated with the Triad Technologies 7 cm (2.5 in) path Brewster angle methane cell in the path. The cell was 100% methane at Denver pressure, and thus contained 70,000 ppm * m of methane. The results are shown in Figures 6 and 7. The results agreed well with the predicted theoretical and previously measured absorption lines for methane.

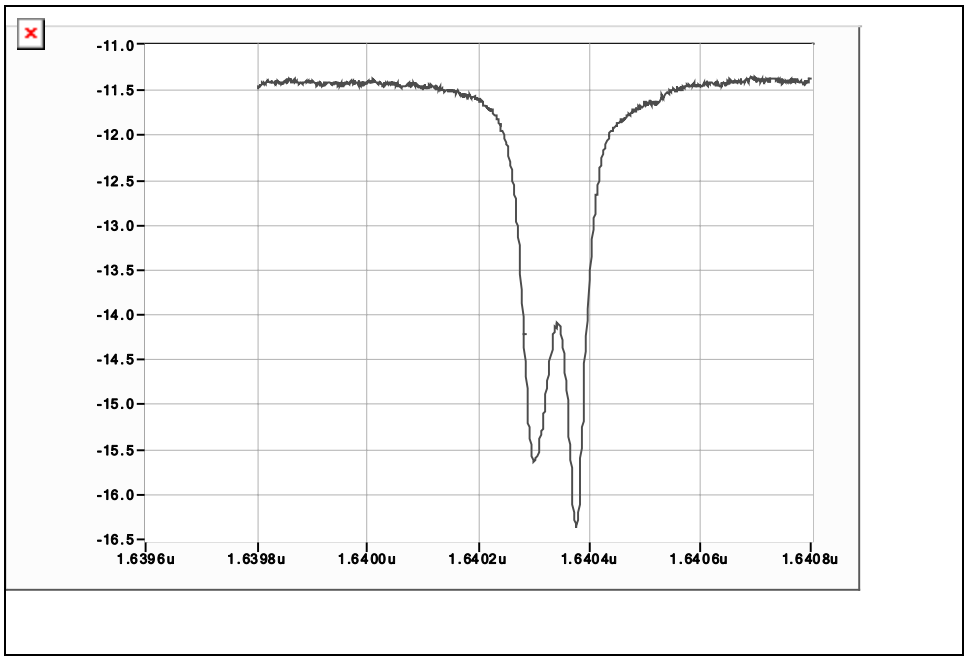

Figure 6. Single Optical Absorption Line for Brewster Angled Windows

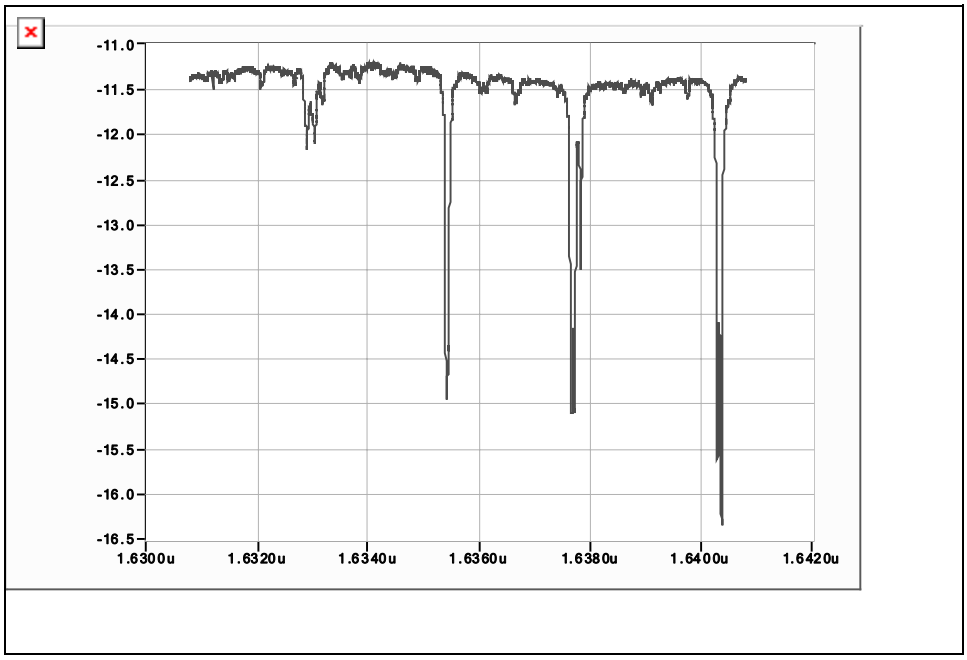

Figure 7. Multiple Optical Absorption Lines for Brewster Angled Windows

The 7 cm pathlength Brewster angled methane cell was now removed, and replaced with the Ophir fabricated variable-fill cell with sapphire windows and a 25.4 cm pathlength. The Ophir cell was empty of methane, filled only with ambient air. The results of these scans are shown in Figures 8 and 9.

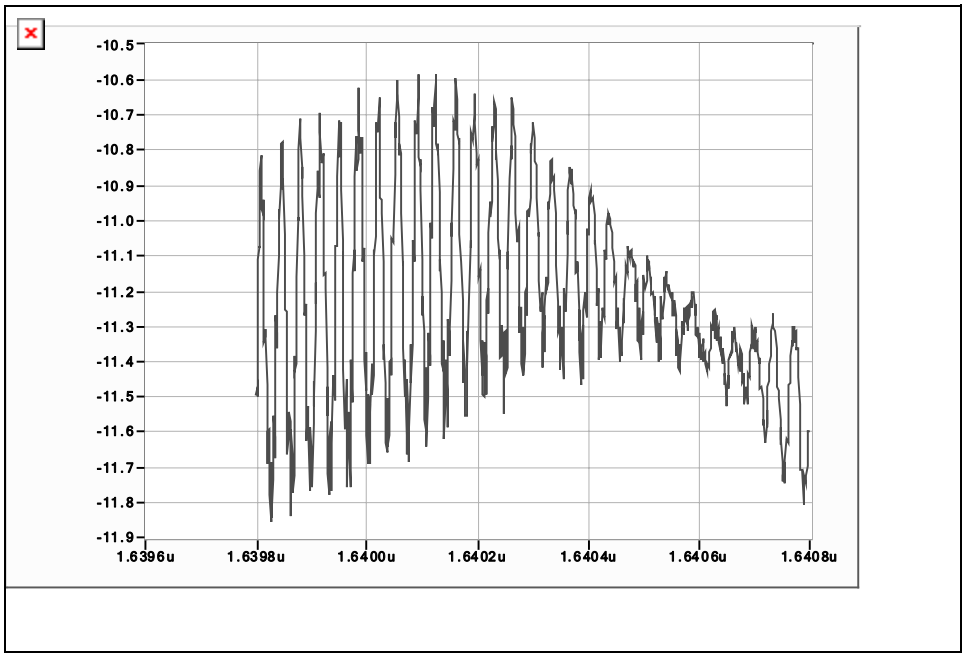

Figure 8. Optical Spectra With Narrowband Scan Through Ophir Variable Fill Gas Cell with Ambient Air Only

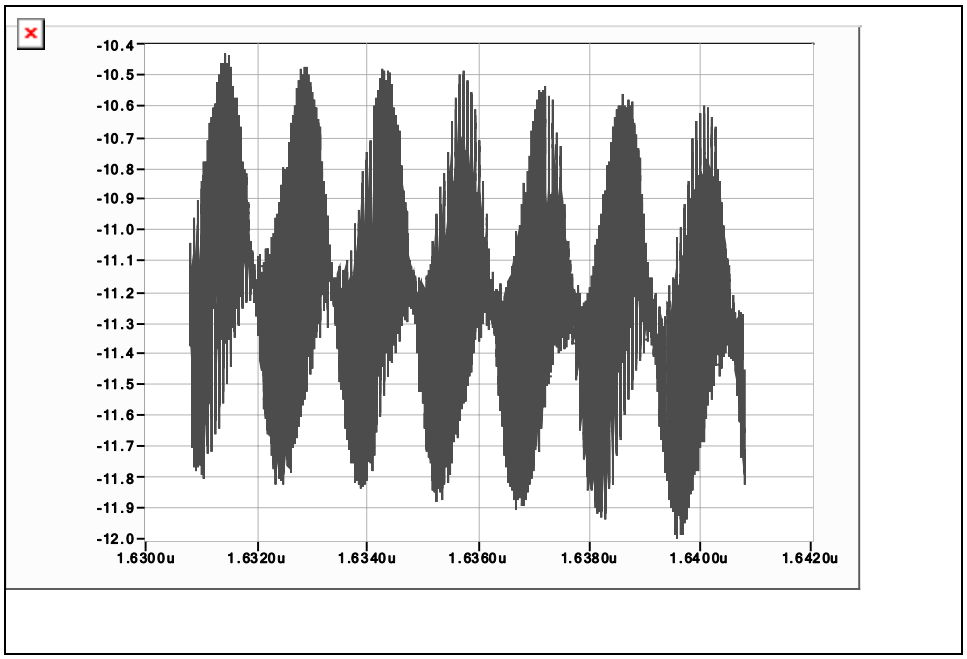

Figure 9. Optical Spectra with Broadband Scan through Ophir Variable Fill Gas Cell with Ambient Air Only

Note that both widely spaced and narrowly spaced sets of etalon fringes were formed. Fringe depth was easily 3 db, large compared to the previously shown methane lines in the Triad gas cell. Apparently low finesse etalon fringes were being formed by constructive and destructive interference caused by bounces both within the parallel faces of the 0.01 mm (0.0004 in) thick windows, and also between the two windows separated by 25.4 cm.

These fringes in the empty Ophir gas cell (with windows nominally parallel to the beam) were very tweaky. They were subject to shifts in wavelength and amplitude when a vacuum was pulled in the tube and when rotating the gas tube. All of these test conditions pointed to the need for closely monitoring the gas cell design. One thing that may help eliminate these etalon fringes is that Ophir is using a fiber amplifier, which produces a much broader output linewidth. The etalon interaction of the broader linewidth with the relatively thin windows should produce less reflections thus minimizing spectral shifts. Erring on the side of caution here probably means at a minimum, angling the windows slightly off of normal. While this does not meet the requirements of a Brewster angle (greatly increasing the gas cell length), the small angle should help with minimizing internal reflections.

2.1.2 Short Optical Path Methane Absorption Testing Using A Narrowband Tunable Laser

First the telescope pair was removed from the setup in Figure 2, resulting in the laser fiber coupled source directly connected to the fiber splitter. A baseline laser scan was

done across the methane absorption lines for the gas cell and blank (no gas) cell optical fiber arms in Figure 2. The results of this scan are shown in Figure 10.

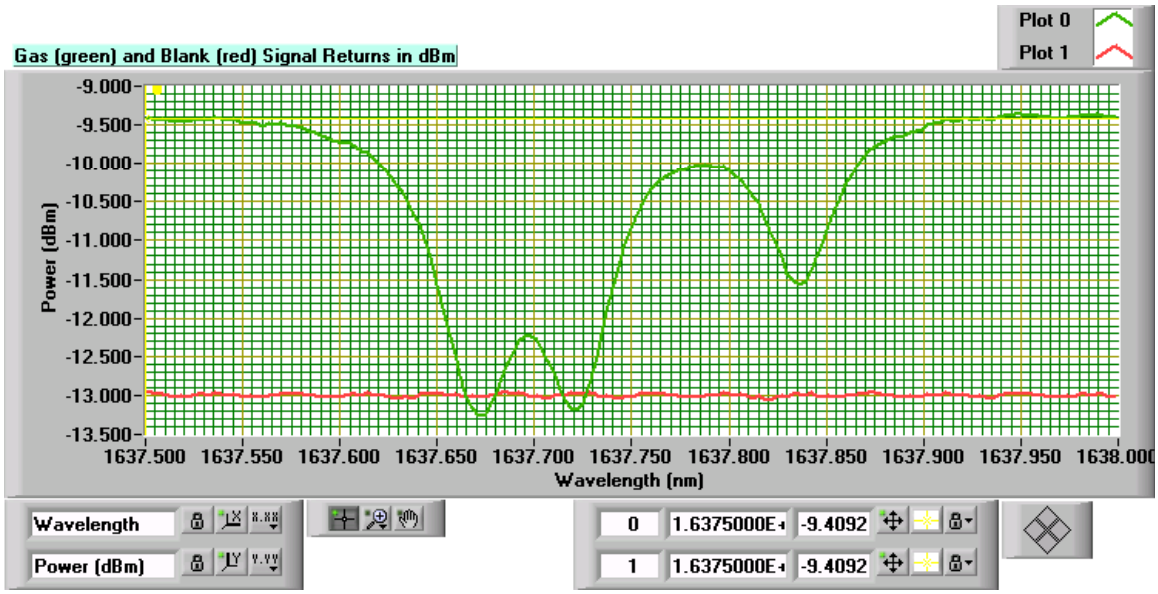

Figure 10. BaselineTunable Laser Scan across Methane Absorption Lines – Green Trace is Raw Absorption Data from Gas Cell and Red Trace is from Blank Cell

Notice the flat absorption seen through the fiber channel with no methane in the path. Transforming the raw data shown in Figure 10 into methane gas concentration was done using the Ophir generated gas correlation algorithms, and is displayed in Figure 11. The gas concentration of the cell or 72,035 ppm * m is shown in the lower left hand corner of Figure 11and agreed closely with the real gas cell concentration of approximately 70,000 ppm * m (99.9 % methane over a 7 cm pathlength). Next, Ophir installed the telescope and receiver optics back into the configuration and measured the gas concentration of the gas cell plus any ambient level of methane to be 72, 621 ppm * m as shown in Figure 12. Even though the signal levels were down by over 50 db in the raw data (not shown), the gas cell concentration was recovered easily. The measured methane gas concentration was slightly higher than was expected, but it was surmised that this was due to the non-optimized noise level of the system. To test this hypothesis, Ophir next injected higher amounts of methane into the optical path.

The gas correlation software should have been able to discern background levels of injected methane from the very high gas cell concentration. This was not the case for these laboratory methane injection tests. There was no increase in the gas-to-blank ratio for the added methane, as has been seen for the previous developed broadband ground based fence-line monitoring radiometer. Subsequent testing did not improve the test results. The differences between the two systems were noted to be the wavelength and the source linewidth, with the newer airborne system having a shorter wavelength and a much shorter linewidth. Optical modeling was initiated using the gas correlation software with a comparable, shorter linewidth, and true to the test results different levels of methane

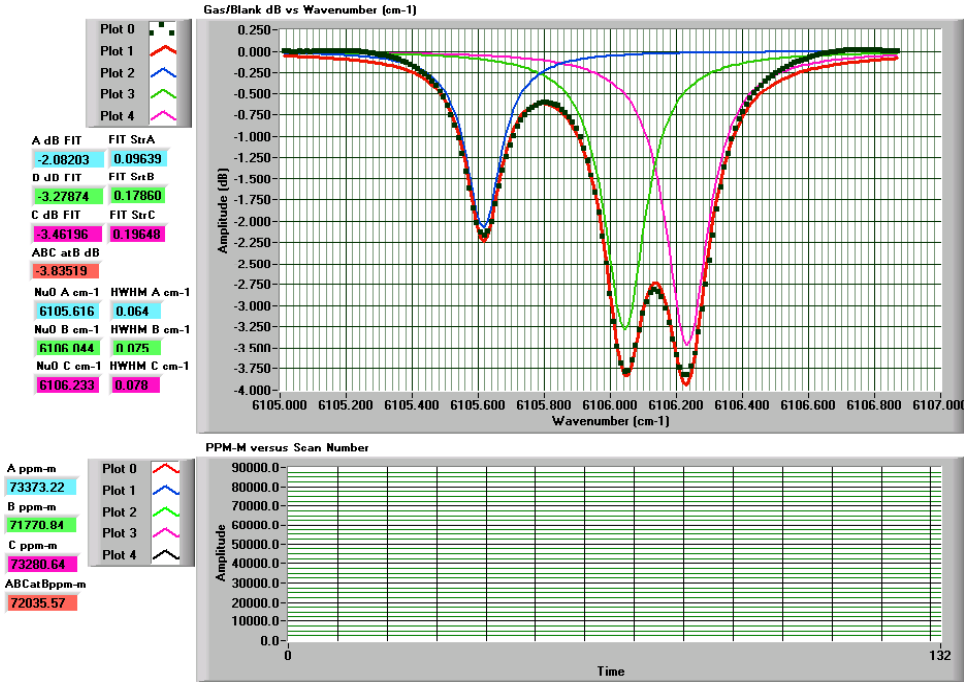

Figure 11. Gas Concentration Data for Methane Gas Cell with 99.9 % Methane for Straight through Fiber Connection

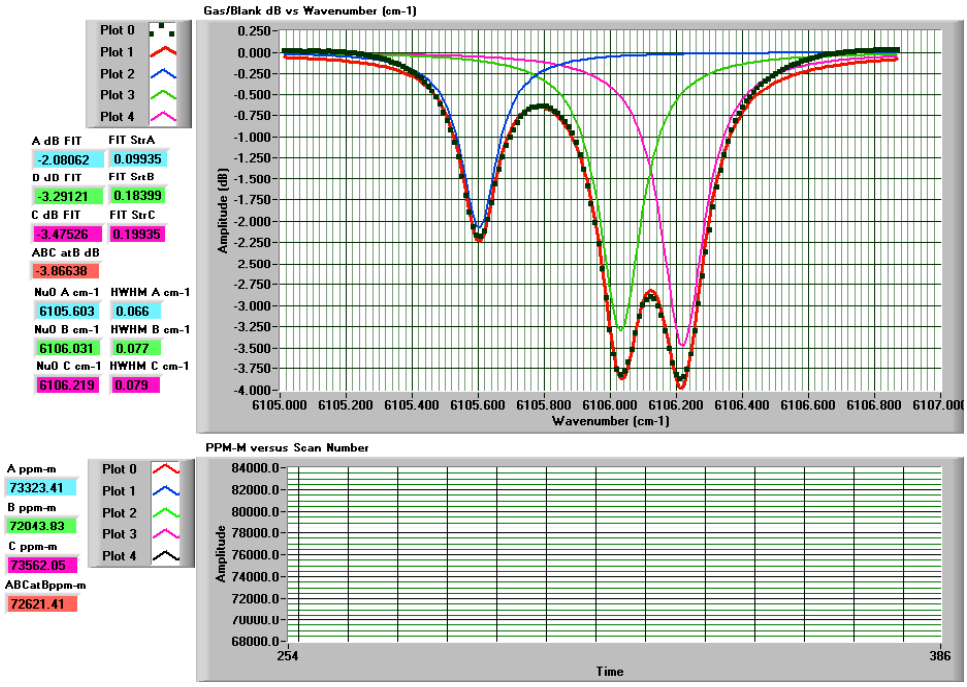

Figure 12. Gas Concentration of Methane Gas Cell Looking at Reflected Light through the Receiver Optics and into the Gas Cell

were not detected. Both the shape and linewidth of the sensing light source greatly impacted the output results of the gas correlation software. The modeling indicated that a broader linewidth as well as a non-gaussian shape was required to detect methane gas concentration levels within the optical path. These models were refined to yield optimum minimal detection levels and these values were transferred to the fiber amplifier vendor as part of the overall parts specifications. From these modeling results, low-level methane detection approaching the background level will be difficult but doable as long as there is tight control of system noise.

The light source vendor has performed their own modeling to verify that they could safely reach the design output goals given the new input requirements, and they have indicated that they can. The final purchase order for the amplifier was completed within weeks of this new specification change.

2.1.3 Results of Target Reflectance Test Using a Large 14-Inch Aperture Telescope and a 1550 nm 1 W Fiber Near-IR Light at 150 m Distance (One Way)

2.1.3.1 Receiving Inspection and Short Range Tests of the Airborne Telescope

Previous reflection tests illustrated the need for larger receiving optics for the airborne sensor. This need was satisfied when Ophir purchased a Celestron commercial 14 –inch aperture telescope. The telescope has a single focusing knob used to move the primary mirror forward and backward, which enables the focal spot to move freely behind the telescope. Ophir spent some time getting familiar with the focusing capabilities of the telescope. It was determined that the closest resolvable focus by the telescope was approximately 47 m (51 ft). The telescope should therefore work well at the airborne optical path distance of 150 m (500 ft).

The telescope was received with a single v-groove rail aligned lengthwise along the telescope. Mounting clamps were purchased separately that mated with the rail and secured the telescope to a flat tripod mount. It was also noted that the telescope had securing screws for the primary mirror that allowed the mirror to be secured once the optimal focus is obtained. These screws can also be removed and replaced with locking hardware adding ruggedness to the mirror mounting hardware. Collimation of the telescope was done at the factory, but if necessary, can be repeated at Ophir's facility using the attached instructions.

2.1.3.2 Initial Reflection Measurements at 150 m

Ophir first worked on establishing the approximate focal point behind the telescope when looking at a target at 150 m. The distance variable was by design set to be 150 m, but the second variable or that of the position of the focusing knob had to be determined. The first attempt at finding the optimal focal point was to view an image behind the telescope using lens paper. The image point was the place where the image was exactly in focus.

This image point unfortunately changed depending upon the setting of the focus knob. Where to initially set the focus knob became the immediate focus of attention. While the telescope in general was designed for use at infinite focus, testing was required to determine the focusing capabilities at shorter distances.

Conversations with the telescope designers allowed us to get a better insight into the optimal focal point for the telescope. They indicated that the telescope was designed to place the optimal focus approximately 4 ″ behind the last optical element or the primary mirror. This corresponds to a point about 2 ″ behind the back optical mounting flange on the telescope. This was the starting point for positioning the light gathering fiber. With the fiber now positioned, the goal was to determine what telescope focus adjustment would yield the maximum amount of energy at the fiber face.

The first series of tests was performed on the night of March 26th, and the initial focus or FOV of the telescope was set to look at a spot 8 ″ in diameter at the target. Flooding the receiving fiber with a visible laser diode source, and then projecting the expanded FOV onto the target helped to set the desired telescope viewing spot size. The corresponding light source spot size was set to be around 3 ″ at the target. Ophir laser radar (lidar) designs have utilized at least a 2:1 FOV overlap with the laser source projection to insure that the laser return does not move out of the FOV, due to vibrations or atmospheric perturbations. The two spots were aligned, using two visible laser diode sources, so that they were centered with respect to each other (additional experiments will be discussed later showing the impact of having the two spots off axis). The visible diode sources were removed from the setup and the near-IR source was connected to the output source fiber optic connector with an output ≈ 500 mW. Power at the detector was measured to be 20 pW, which was substantially less power than expected.

The power reflected back to the receiving optics was obviously much less than predicted, given that previous testing had predicted at least three orders magnitude higher return. In order to improve the signal return, Ophir experimented with the focus adjustment on the telescope anticipating that the focus onto the fiber may have been slightly off. Finding the optimum focus onto the fiber increased the signal at the detector to just over 500 pW. While changing the telescope focus showed a large improvement, the overall signal return was still less than expected. Two areas of concern were seen by Ophir to be the most likely contributor to the lack of signal return; the first was the inability to focus the entire signal onto the small 62.5 μm fiber core and second, the impact of the telescope secondary mirror obscuration on the signal return.

2.1.3.2.1 Development of Models for 14-Inch Schmidt-Cassegrain Telescope Showing Minimal Focus and Corrector Plate Performance Characteristics

Prior to purchasing the telescope, Ophir generated models during this performance period that indicated the Celestron telescope had the ability to focus the reflected light onto a very small spot. The model was developed to help explain the optical performance characteristics of a Schmidt-Cassegrain Telescope (SCT) with and without the corrector plate, using Zemax ray tracing software. The calculations included encircled energy calculations at prime focus, which would give an estimate of the total amount of energy

that could be coupled into the multimode 62.5 μm optical fiber placed at the focal plane. The Zemax calculations also included comparisons to the best-possible, diffraction-limited optical performance. While Ophir did not posses detailed information regarding the Celestron telescope design prescription, all SCT's have a number of optical elements in common as shown in Figure 13. This configuration closely approximates the Celestron SCT. The telescope prescription for the model was optimized to produce a diffraction-limited beam spot at the focal place for a single wavelength, at 550 nm. The performance of the optical system was then characterized by encircled energy calculations at the focal plane. The light wavelength was then shifted from 550 nm to 1650 nm and energy encircled calculations at focus were reproduced. At 1650 nm, the image plane from prime focus was moved and new encircled energy calculations were produced to get an idea of the light-coupling tolerance, hence potential vibration sensitivity, of light coupling into the multimode optical fiber. All of these calculations were based upon infinite focus or parallel light rays into the telescope. The inclination angle was also assumed to be 0 degrees. The modeling results for 550 nm light are summarized in Figures 14 and 15. For 550 nm, the actual and diffraction limited optical performance was virtually identical. Better than 90% of the available optical power was within the 62.5 μm fiber diameter.

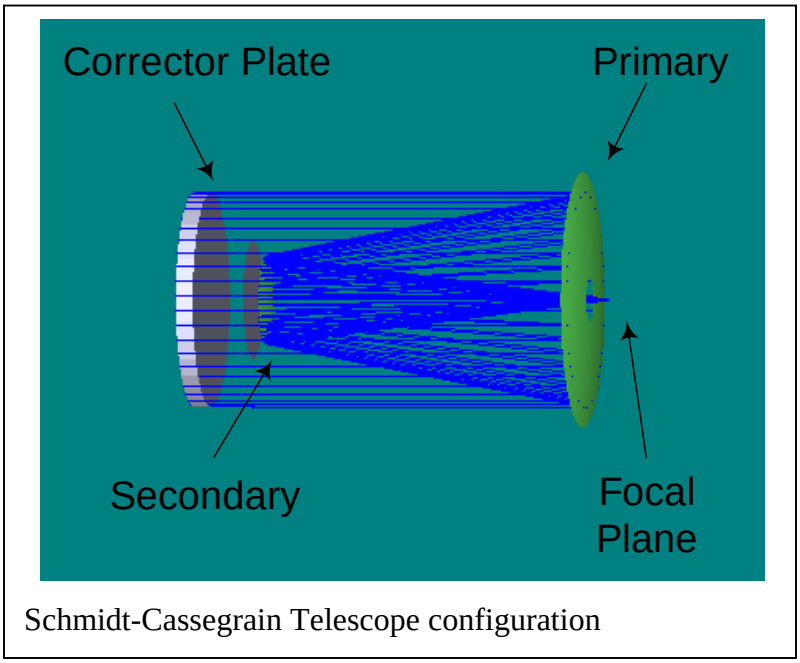

Figure 13. Schmidt-Cassegrain Telescope Configuration Used in Zemax Models

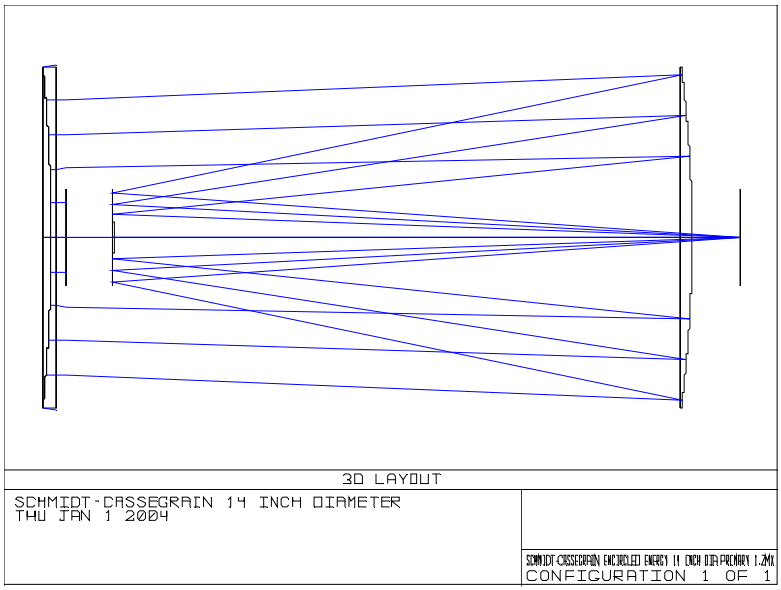

Figure 14. Ray Trace at 550 nm with Object at Infinity

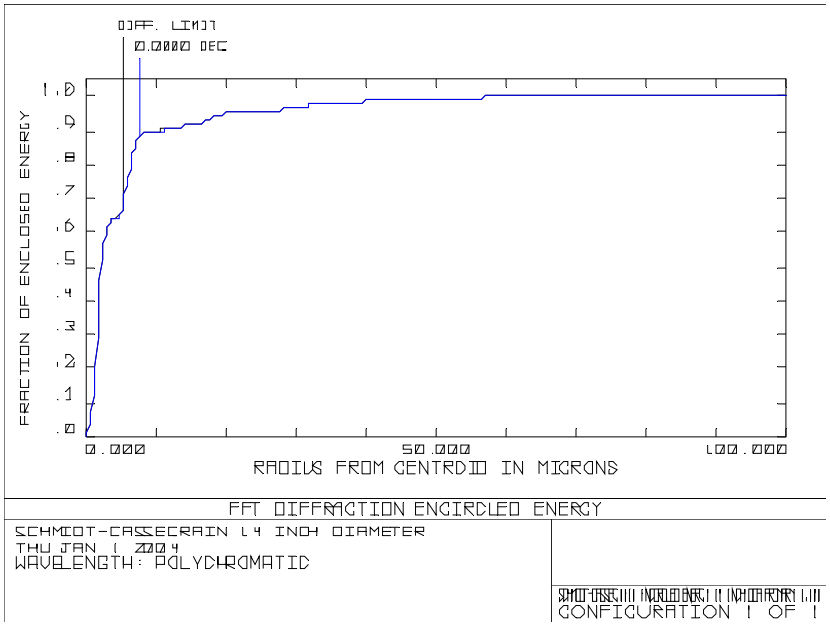

Figure 15. Encircled Energy Calculation at Prime Focus for 550 nm Light

The wavelength was then changed to 1650 nm, and the optimal focal position distance was changed to correct for corrector plate dispersion. Encircled energy calculations at 1650 nm were completed and are shown in Figure 16.

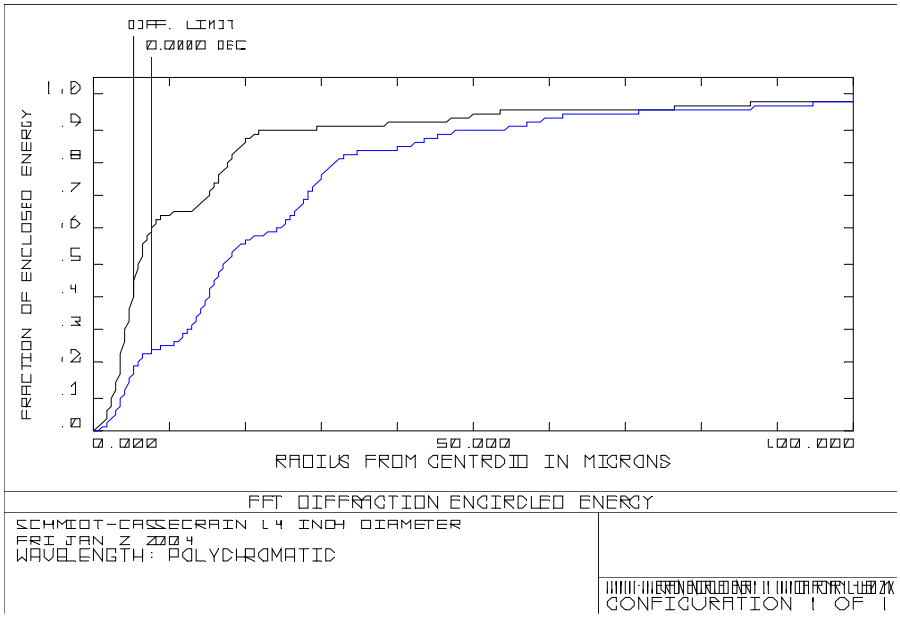

Figure 16. Encircled Energy Calculation at 1650 nm, Calculated at New Prime Focus Position

The new prime focus for the data shown in Figure 16 was 40 mm closer to the telescope primary mirror from the prime focus seen for the 550 nm light. The multimode fiber coupling efficiency was approximately 78% for the 1650 nm plot therefore it would be expected in real life to be down in efficiency by about 10-12 %, when gathering near-IR light with the SCT. Moving the image plane away from the prime focus 60 –120 μm caused a relatively small loss of 2-3 % in coupling efficiency, which helped to alleviate fears of large losses due to slight movement in the fiber.

The Zemax models also helped Ophir to understand the benefits of using the corrector plate in the SCT. The corrector plate looks to be the weakest element of the telescope structurally speaking. Without the corrector plate the models indicated that the telescope in the normal two-mirror configuration would not be able to focus the light adequately. The Fastar configuration (secondary mirror removed) lessens the F# of the telescope, potentially increasing the light gathering capability of the telescope but increases the difficulty with mounting of the detector optics in front of the telescope. The lower F#2 of the telescope also requires a larger fiber numerical aperture than currently exist with the 62.5 μm fiber.

2.1.3.2.2 Further Analysis of SCT Focusing Performance

The results of the initial target reflectance testing at 150 m were disappointing and did not agree well with the anticipated signal return. Previous signal reflection measurements done with smaller optics at shorter optical pathlengths indicated that the larger telescope would have a 7X increase in receiving power, when adjusted for the

signal return loss due to the $1/r^2$ rolloff where r is the optical pathlength. In rough terms, the large telescope should have yielded slightly less power at 150 m as did the smaller optic at 50 m. This was clearly not the case with the large telescope, as it yielded only a few percent of anticipated signal return.

Ophir began to question the modeling analysis, as it did not explain the actual system performance. The modeling was performed using the assumption that the return light entered the telescope from an infinite focus distance or entered as parallel light rays (Zemax software was incapable of using any other object focus distance). The fact that the light rays enter the telescope as non-parallel rays may have masked the problem with focusing of the image. The lens equation is defined as equation (1) and using it to evaluate the image and object sizes of the optical system may shed some insight into the lack of system performance.

$$1/s' = 1/s + 1/f \qquad (1)$$

where s' is the image distance, s is the object distance and f is the focal distance.

In the test configuration, the object distance = 150 m, the focal distance of the telescope = 3.91 m and the image distance is unknown. Substituting these numbers into (1) and solving for s yields s = 3.81218 m. The magnification of the system is defined by equation (2).

$$M = s' / s \qquad (2)$$

The magnification of our system is therefore 3.81218 / 150 or .0254. For a fiber with receiver core size of 62.5 μm, the maximum object size is only 62.5 μm / .0254 or 0.246 cm (0.1 in). In other words, the FOV of the telescope at 150 m is restricted to 0.246 cm (0.1 in) when trying to focus the light onto a 62.5 μm fiber. This may explain why only a small fraction of the available light energy striking the target was reflected back to the telescope (remembering that the light source was focused to a 10 cm (2 in) spot on the target). One way to compensate for this effect would be to shrink the light source spot size at the target, a second way would be to increase the fiber core size; lowering the F # would shorten the focal distance effectively increasing magnification. For example, increasing the fiber core size to 1000 μm, increased the magnification by a factor of 16 which changed the acceptable object size to 4.1 cm (1.6 in). Results of incorporating these improvements into the test configuration will be described in a later section.

2.1.3.2.3 Analysis of the Impact of Secondary Mirror Obscuration on Signal Return

At an infinite distance, the secondary mirror obscuration will act to reduce the overall signal through the telescope by the ratio of the area of the obscuration (102.6 cm^2 or 15.9 in^2) to the area of the telescope aperture (993.1 cm^2 or 154 in^2) or by approximately 10%. As the optical distance decreases, the impact of the obscuration is more and more pronounced. In an attempt to further quantify the obscuration losses at 150 m, Ophir calculated theoretical losses due to the obscuration at 150 m using some existing laser radar (lidar) analysis software. This proprietary software had been used to calculate backscatter off of aerosols at various optical distances, but was manipulated to determine

the reflected signal off of a hard target at 150 m. The output light source beam size was set to 5 cm (2 in), the center obscuration was 11.4 cm (4.5 in), and various fiber diameters were modeled. The output from this lidar return model is summarized in Figures 17 and 18, and showed the calculated signal return and the telescope to laser overlap, for 62.5 and 1000 μm optical fibers. In both of these Figures, it was obvious that the larger fiber saw the least impact in signal reduction from both relative return power and signal overlap. Signal overlap was the most impacted by the short optical pathlength, with very little of the signal getting back to the detector.

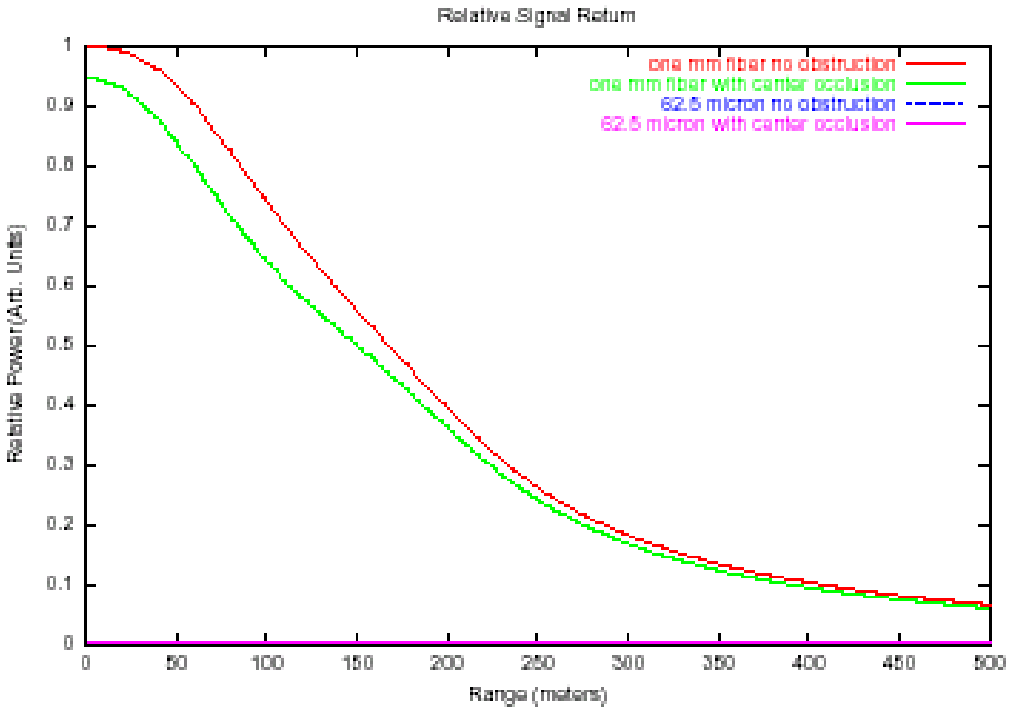

Figure 17. Modeled Signal Return for a 14-Inch Telescope Using 62.5 Micron and 1000 Micron Optical Fiber Core with and without a Secondary Mirror Obstruction

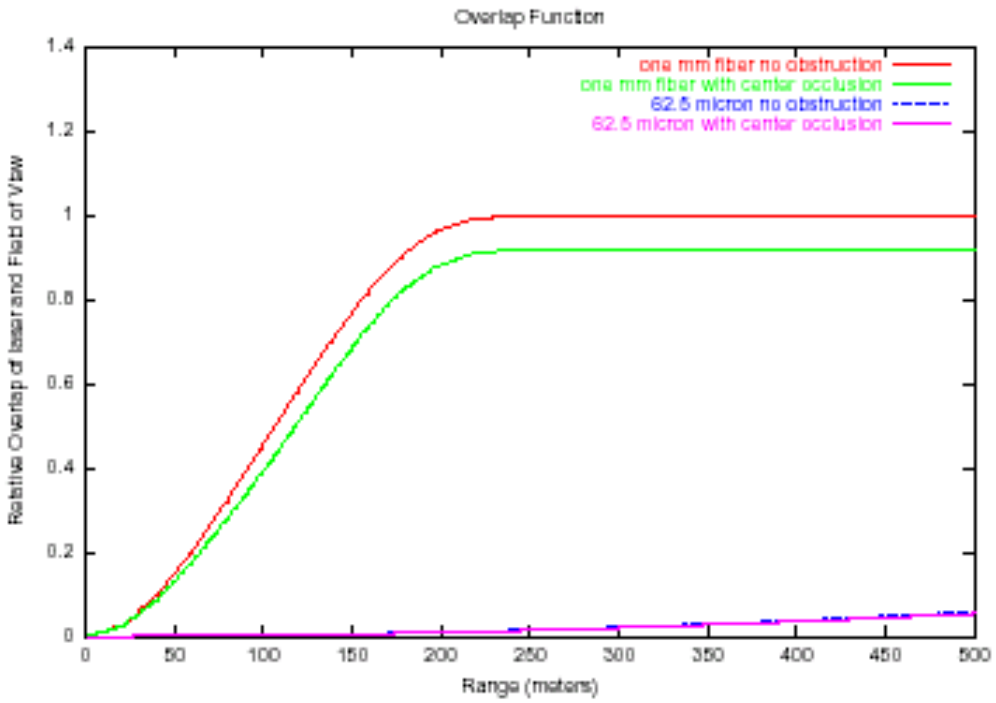

Figure 18. Modeled Signal Overlap of Laser and Telescope FOV Using 62.5 Micron and 1000 Micron Optical Fiber Core with and without a Telescope Occlusion

2.1.3.3 Second Series of Target Reflectance Test at 150 m

Ophir determined from the signal modeling that increasing the fiber core size would likely increase the signal return and increase the telescope overlap at 150 m, both favorable to increasing the signal at the detector. At this time, Ophir placed an order for larger core multimode fiber from 100 to 1000 μm. Prior to receiving this fiber, Ophir continued with the outdoor target reflectance testing a second evening on April 9th, using the setup in Figure 3 with a few modifications. The first goal of this test was to use a focal reducer of F# 3.3 in front of the optical fiber to reduce the focused spot size at the fiber by reducing the overall system F#. Classic radiometry states that the energy back to a detector is inversely proportional to the square of the F#. Using this as a baseline, it can be seen that going from an F# 11 to an F# 3.3 would yield a tenfold order of magnitude gain in signal at the fiber. In reality, the gain in signal at the detector increased by a lesser amount or 3-4 times (≅ 65 pW). The focus through the reducer was optimized to obtain the maximum signal. This spot size at the target was approximately 1.25 cm (0.5 in), which agreed fairly well with the calculated spot size obtained from using equation 2 to find the optimum magnification. The focal reducer helped to show that indeed decreasing the focus spot aided in signal detection. It should be noted that the conditions for this test were less than ideal with a steady rain falling during the test. (It has already been shown that wet surfaces are poor reflectors in the near-IR region and that large aerosols such as raindrops can drastically alter the light path by scattering the light before it intercepts the target). The power at the detector was less than a tenth of the return seen during the test on March 26th, even with the focal reducer in the configuration.

It should be noted that during this last test measurement, the size of the laser spot at the target was seen to vary greatly depending upon the source wavelength. It had been assumed that once the laser spot using the visible light was fixed, the spot size would not change when changing over to the 1550 nm near-IR source. This was not the case and from here on in the test setup, the laser spot size was rechecked every time the source wavelength was changed.

The signal overlap models indicated that using the 62.5 μm fiber yielded a very poor overlap at 150 m. Changing the alignment parameter in the model from an on-axis to an off-axis configuration, yielded slightly more energy at the detector especially when using larger fiber. With the focal reducer in the configuration, data was gathered to determine the impact of moving the laser spot off-axis (non-centered) with the telescope FOV. Using the same spot sizes for the laser and the telescope FOV, the laser spot was moved outside the telescope obscuration. In order to locate the obscuration against the laser spot on the target, the focal reducer was removed and the telescope was flooded with visible light (the FOV was much larger without the focal reducer). Once the laser spot was shifted, the focus behind the telescope had to be optimized again since the focal spot was off-axis with the telescope line-of-sight. This realignment was performed using an X-Y optical adjustment stage, which moved the fiber to the appropriate off-axis focus position. The optimal energy at the detector measured 65 pW, which was the same as was seen in the on-axis focal reducer configuration. It should be noted that the telescope FOV was only 0.5 ″ in diameter using the focal reducer and moving the spot around against a 2 ″ laser focus spot probably was not an accurate test for the off-axis gain. The fact that the energy did not change probably meant that we were still sampling return from the laser spot, only at a different portion of the spot. Assuming uniform energy density across the laser spot at the target, one would assume with the same telescope FOV size that equal amounts of energy would be measured (as was seen). A more useful test would be to make the telescope FOV larger than the laser spot. The obscuration would be more easily discernable on the target. The only problem with this setup was that the telescope would not be at optimal focus and the energy would be much less at the fiber. Clearly, this test was hard to perform with the small fiber. More testing is required using the large core fiber to determine if signal gain can be seen with an off-axis laser source.

Given the much smaller than anticipated signal measurements, it was decided to perform a comparison of the airborne telescope to the smaller transmitting optic with a smaller F#. The setup in Figure 3 was modified by replacing the 14-inch SCT with a smaller 2-inch transmitting optic, identical to the receiving optic used in the 50 m target reflectance test during the previous performance period. Standard multimode 62.5 μm core fiber cable was used. The receiver optic and the laser output optic were co-aligned and centered with the laser spot size set to 5 cm (2 in) in diameter. The receiver FOV was set to the smallest size possible at the target or 45 cm (18 in). The amount of signal at the detector was 135 pW or twice the energy captured by the larger telescope. Theoretically, the solid angle of the larger telescope should have contributed to larger signal return, unless there was some other factor limiting the signal collection i.e. limiting profile of optical fiber. Even though the smaller optic worked at least as well at gathering return signal, the amount was still well under the signal required for sufficient signal to noise. It was

becoming more obvious that the use of the small fiber with the larger F# telescope was the single largest limiting factor of the signal return at the detector.

2.1.3.4 Third Series of Target Reflectance Test at 150 m

On April 27th the third in a series of reflectance tests was performed. Most of the test data gathered was centered on using various larger core optical fibers as the interface from the large telescope to the detector. In order to use the larger core fiber, a larger area detector with an active diameter of 5 mm was used. The low noise detectors used up to this time were restricted to an input fiber core diameter of less than 100 μm. The larger area detectors have an electro-optical noise floor of around 5 pW compared to less than 0.3 pW for the low-noise detectors. It was anticipated that although the large area detectors are "noisier" by an order of magnitude, the amount of signal gain would increase by several orders of magnitude.

2.1.3.4.1 Preliminary Indoor Laboratory Reflectance Measurements Using Large Core Optical Fibers and Large Area Detector

Ophir conducted some preliminary tests inside the laboratory, just prior to setting up outside, using the smaller transmitting and receiving 2-inch optics, the high output source and the larger optical fibers. Table 1 summarized the target reflection results off of a diffuse painted wall at 10 m (33 ft) optical path. The results were quite promising as they indicated a significant gain in signal with increasing fiber core size. The largest gain was seen when using the 1000 μm fiber, as expected. The signal gain was 157X when going from the 62.5 to 1000 μm fiber. It turned out that 1000 μm core fibers are the largest practical commercially available fiber on the market. Optical fibers larger than this are costly, inflexible and hard to use. The connector terminations are also limited. Ophir has chosen the FC/PC connectors due to their availability and ease of use, and FC/PC connectors are limited to core sizes of just slightly larger than 1000 μm.

Optical Fiber Core Size, in μm	Core to Cladding Transition	Measured Power at Detector, in nW
62.5	Graded Index	7
100	Graded Index	15
105	Step Index	22
300	Step Index	140
600	Step Index	700
1000	Step Index	1100

Table 1. Indoor Reflectance Measurements Against a Diffuse Painted Wall at 10 m Using 2-Inch Optic, Near-IR Source with Optical Power at 400 mW and Large Area Detectors

It should be noted that the step index fibers appeared to be somewhat more efficient at coupling light than the graded index fibers. This agreed with the findings of Hobbs[2000] that step index grading allowed for better air to core light coupling than graded index fiber.

2.1.3.4.2 Outdoor Target Reflectance Measurements Using Large Core Optical Fibers and Large Area Detector

The setup remained the same as shown in Figure 3 with the exception of the Agilent Model 88634A detector, which was replaced with a Model 81624A large area detector. The multimode 62.5 μm detector fiber was also eventually replaced with several fibers of larger core sizes. The large telescope was used as the receiver and the light source was focused with the 1 ″ transmitting optic with a focal length of 40 mm. The weather conditions for this test were warm, clear and low humidity.

The power output of the 1550 nm fiber amplifier was set at approximately 500 mW with the Pump #1 drive current set to 0.81 A and the Pump #2 drive current set to 0.56 A. These test conditions were held constant throughout the evening of testing. The Spectralon highly reflective target was used for all of the reflective measurements.

A variety of optical fibers including 100 μm graded index, 105 μm step index, 300 μm step index, 600 μm step index, and 1000 μm step index were used as receiver interfaces from the telescope to the large area detector. The fiber adapters at the telescope and the detector were drilled out to accommodate the large core fibers. As explained before, the FC/PC style connectors were designed to handle up to just slightly larger than 1000 μm fiber core, if the coupling “end” ferrule is drilled out. The alignment process was the same for each fiber test and can be summarized as follows:

- The telescope and the light source optic were co-aligned using fiber coupled, visible red laser diode sources to flood the optics. The light source spot size at

the 150 m target was focused down to 5 cm (2 in) and the telescope FOV was optimized by focusing the telescope down to the tightest focus possible at the target. The optimal FOV at the target increased with increasing fiber core size indicating that the acceptable object size had increased.

- Next, the two spots were centered directly over each other at the target using the visible sources.
- The near-IR 1550 nm source was connected to the light source optic to insure that the location and spot size was acceptable (the location was marked on the target). It was noted earlier that the transmitting optic produced different spot sizes for different wavelength sources.
- The telescope was flooded with the near-IR source and the FOV was checked to make sure that it was still optimized and centered with the light source spot.
- The single mode fiber was connected from the fiber amplifier to the light source fiber adapter.
- The multimode large core fiber starting with the 1000 μm fiber was connected from the telescope fiber adapter to the large area detector.
- The fiber amplifier was powered up to the prescribed output power.
- The telescope FOV was fine-tuned to yield the maximum power at the detector. This step usually required only a small amount of refocusing.

Table 2 summarizes the signal reflection data taken for different large core fibers.

Optical Fiber Core Size, in μm	Core to Cladding Transition	Measured Power at Detector, in nW	Field-of-View Diameter at Target
100	Graded Index	1.5	Not Taken
105	Step Index	1.5	0.875 Inches
300	Step Index	12	0.625 Inches
600	Step Index	50	1~1.25 Inches
1000	Step Index	165	1.25~1.5 Inches

Table 2. Detector Power Measurements Taken with Target at 150 m Distance Using Large Core Fibers

Increasing the fiber core definitely increased the amount of signal collected through the telescope and into the detector. A gain of hundred fold was seen when going from the 100 μm fiber to the 1000 μm fiber, which roughly corresponds to the ratio of the areas of

the fiber core. Larger fiber might yield even higher signal return, but the practical limitations of using large core fiber limit the size to around 1000 μm.

In order to determine the impact on signal return of varying the FOV of the telescope away from the optimal size, the FOV of the telescope during the 1000 μm was increased to 4 ″ or roughly twice the size of the light source spot. The new power measurement at the detector was 38 nW, which was dramatically less than seen for optimal focus. This further strengthens the argument to fix the telescope at minimum focus.

Further testing will be performed to determine the impact of shrinking the laser spot in relation to the telescope FOV. On the surface, it would appear that if the entire laser spot was contained within the FOV that more energy would be transferred through the telescope. Recent preliminary tests have shown that this idea may not have shown any increase in the signal at the detector. More details will be forthcoming in the next summary report.

2.2 Transceiver Design Results

2.2.1 Selection of Transceiver Light Source

Ophir continued to devote a great deal of time during this performance period to the development of the design specifications required for the airborne system light source. From past experience, Ophir has relied heavily on well-developed design specifications especially when developing and designing a novel, custom part. After reviewing different technologies capable of producing high output sources in the 1600 – 1700 nm wavelength range, Ophir has decided to proceed with the design and development of a highly non-linear fiber amplifier. The groundwork had been laid during the previous performance period in establishing a good working relationship with a highly non-linear fiber (HLNF) amplifier vendor. Numerous months of cooperative work went into the development of the overall design specifications. The design specifications addressed issues such as source modulation, center wavelength stability, center wavelength tuning rate and range, spectral output linewidth, averaged output power, seed source characteristics, output ripple, required warm-up time, amplifier output signal to noise ratio, optical polarization requirements, output power stability, software interface, and mechanical format. The specifications were in a continual state of change until the beginning of January 2004, when they were finally locked down. Potential design problems with HLNF amplifiers such as Brillouin scattering were addressed one-by-one either with actual testing, model simulations or past design similarity comparisons. The vendor was put on contract for the amplifier in mid January and is scheduled to deliver the part by June 26th. The vendor is providing Ophir with end of the month updates, as well as helpful software interface information on an “as available basis”.

2.2.2 Transceiver Telescope Design

Past target reflection measurements from a target a 50 m distance indicated that larger optics (> 2-inch optics) would be required to meet the signal to noise requirements, when looking at the ground from an airborne system at 150 m altitude. The signal drops off

inversely proportional to the square of the target distance. From 50 to 150 m, the signal to the detector is expected to decrease an order of magnitude or 10 fold. At a minimum, Ophir determined that an 8-inch optic would be required to yield equivalent performance specifications at 150 m. Commercial telescopes were readily available with apertures of 8, 11 and 14 inches. The SCT has the advantage of a shorter optical focal length and is often the choice of astronomers for this reason. The airplanes that Ophir has access to for use as a flight platform all have height space restrictions in the cabin, so the SCT design was selected.

Ophir acquired a "loaner" 11-inch aperture telescope from Celestron to evaluate design concerns such as ruggedness and light transmission in the near-IR wavelength range. This model had the Starbright XLT coating, which is an upgrade and has slightly higher transmission. The XLT package has better coatings and a better corrector plate (made of white water glass). Directing a near-IR beam at 1550 nm into the telescope showed that the light transmission was 20% less than the advertised throughput for the visible wavelengths or about 60 % overall transmission. The visually clear corrector plate near the end of the telescope was probably the optic contributing to the highest transmission loss. Without the corrector plate, the telescope does not have the ability to focus the incoming light. It also acts to correct for spherical aberrations at the image plane.

As a result of the transmission testing through the "loaner" telescope, Ophir decided to order the larger 14-inch model with the XLT upgrade package. While the telescope may be somewhat larger than required, the large aperture should help to offset optical losses through the corrector plate. A picture of the telescope being used in a test setup is shown in Figure 19.

Figure 19. Photograph Showing Outdoor Test Setup of Co-Aligned Transceiver with 14-Inch Telescope and 2-Inch Laser Source Optic

2.2.3 Transceiver Mounting Hardware Design

The telescope and the light source transmitting optics were co-aligned to a certain stare point or target. Optimally, the two should be aligned along the same axis, with the light source located at the exact center height of the primary and secondary mirrors of the telescope. The advantage to this design is that the telescope and the source optic can be pointed at any target, regardless of the distance and still be aligned with each other. This was the configuration adopted by Ophir. The limiting dimension of this configuration was the overall length, since the optics are mounted in-line with each other. The length has to fall within the constraints of the cabin height of the small airplane chosen for the flight test.

Earlier in the project, Ophir had hoped to use the company owned Beechcraft Bonanza as the airborne platform. Ophir intended on pointing the transceiver out the open side doors and surveying the pipelines at a non-normal angle. Unfortunately, the reflection testing done during the previous performance period showed that a downward looking belly hole in the airplane was by far the best choice. Losses of 60-70 % of the reflected signal could be expected from a transceiver-target configuration mounted off-axis by 45 °, as in the side exit Bonanza doors. The decision was made to locate possible lease aircraft in the Denver area that have flight-test certified belly viewing holes. The most popular and most cost effective airplanes that met this requirement were the Cessna Model(s) 206 and 207. The Model 207 is a stretched version of the Model 206 with a slightly larger engine and is capable of safely carrying more weight. They both have good control and performance at airspeeds below 100 mph, making them ideal for slow pipeline inspections.

Ophir has located and visited two companies that routinely lease out these Cessna Models. Since these visits, Ophir was notified that one of these companies had decided to sell their airplane and can no longer guarantee it's availability over the summer. In order to head off the possibility of not having an airplane available when it was needed, Ophir has worked out an arrangement with the other company, Aero Systems, Inc. of Erie, Colorado, reserving the Cessna Model 207 on a monthly or weekly basis beginning in July. The leasing arrangement and cost are much more attractive than with the previous lease company. Aero Systems, Inc. has been quite helpful in supplying us with drawings of the cabin area where the belly hole is located. They are currently flying a contractor supplied lidar system on this airplane and have notified the company of our proposed flight schedule. One nice feature about this arrangement is that if Ophir by chance isn't ready to fly by July 1, Ophir will be given the option of sliding the schedule out as long as it notifies Aero Systems a month in advance. It sounds like the lidar developer would willingly use any available flight time during the summer months. Currently, Ophir is evaluating the status of the program and will make a decision within the next few weeks concerning the flight test schedule.

During the airport visit to Aero Systems, Ophir spent some time comparing the drawings to the actual aircraft and taking reference photographs. Photographs of the Model 207 interior are shown in Figures 20 and 21. The lidar system is shown covered by a black plastic bag and is located directly above the belly hole. The aircraft has existing mounting shock absorbers within the belly hole, which appear to be well suited for

mounting of the optical transceiver. The lidar system was still mounted into the cabin when Ophir inspected the airplane. The weight and size of the lidar system was very close to the proposed weight and size of the optical transceiver, so Ophir felt very confident in using the existing mounts. The lidar system also used a 19-inch chassis rack nearly identical to the rack that Ophir will use in the airplane. One remaining unknown is where to sit the computer operator during the flight test? The photograph in Figure 21 illustrates the close proximity of the pilot's seat to the 19-inch computer rack. There currently is a small spot behind the pilot for an operator to sit, but it is cramped. A second visit to the facility will be required to better determine the logistics of mounting the system in the airplane. One critical dimension that Ophir needs to work with closely is the interior cabin height, which is 42 ″ from floor to ceiling. The transceiver could be dropped into the belly hole to gain another 2 – 3 ″, giving a total vertical height of 44 ″. The 14-inch optical tube length is 31 ″, the light source focusing optic may be as much as 7 ″ long and the optical fiber bend radius for two cables will probably be 6 ″, yielding a combined length of 44 ″. The current design will push the available height, but it may be possible to reduce the focusing optic length down to a couple inches, if the spot at the target can be focused down to less than one-inch in diameter (upcoming outdoor test will verify this data).

Figure 20. Photograph of Cessna Model 207 Side Cabin View

Figure 21. Photograph Showing Cessna Cabin View from Position of Co-Pilot Seat (Seat was Currently Removed for Current Flight Test)

The transceiver hardware consists of the telescope, laser source focusing optic, telescope mounting rails, fiber optic mounting adapters, mounting plate, and three vertical mounting rails. The vertical height of the rails will be close to the maximum height of the cabin. These rails are made of extruded aluminum with lengthwise slots for attaching optical mounting hardware. The telescope is attached to two "v-groove" rails running lengthwise, which are mounted to four heavy-duty clamps that are bolted to the extruded rails. The whole assembly will be bolted to a large aluminum plate and dropped into the belly hole recess, where the shock mounts are located.

The fiber amplifier has been designed to fit into a 19-inch rack similar in size and location to the one shown in the foreground of the photograph in Figure 21. The amplifier is fiber coupled to the transceiver through a single mode SMF-28 fiber cable. The receiving large core multimode fiber is attached to a fiber adapter mounted at the focal point of the telescope and is routed to external optical detectors located within the 19-inch rack. The entire operating system for the system will reside on a ruggedized laptop computer situated on a slide out shelf within the rack.

2.2.4 Optical Detectors

Ophir has experimented with using large core optical fibers (up to 1000 μm) in the receiver optical path, and has seen much better light coupling into the large area detector. The Agilent Model 81624A large area detector is very similar to the Agilent Model 81634 detector described in the previous summary report. They both interface with the Agilent Optical Mainframe, have similar data transfer characteristics, are sensitive over the same wavelength range, have the same averaging time of 100 μs, and operate over the same temperature range. The key differences reside in the type of fiber input they will accept and the noise levels. The large area detector has the ability to accept large core fiber, whereas the 81634 detector is limited to fibers with cores up to 100 μm. The trade-off is in the area of noise levels. The large area detector has a dark noise level that is roughly 25 times that of the 81634 detector or about 5 pW. Recent reflectance data has indicated that the amount of reflected light hitting the large core fiber is up to 100 times greater than with the standard multimode fiber. So in the end, it seems that we are gaining more signal than we are gaining noise, and the resulting signal to noise level goes up. Some of the earlier problems with light leakage into the fiber may become less of an issue, if the power received by the detector is many times higher than the observed leakage.

2.2.5 Optical Filters

The fabrication of the optical filters is a two-stage process, involving two different vendors. The optical filter substrates have been ordered and delivered to Ophir by Barr Associates. One filter has been built with the methane-sensing wavelength as the center transmission wavelength and the other has been built with the ethane-sensing wavelength as the center. Both of these filters have been designed to highly reject the other center wavelength, and the desired light is therefore passed through to the detector. The filters also have very good blocking characteristics of all visible light or in particular solar background light, adding to optical noise rejection. A second vendor will take the filter substrates and package them into a fiber-coupled package. This vendor has responded with a quote for the smaller standard multimode fiber, and has verbally responded that there should be no “show stoppers” with increasing the fiber input to larger core fiber.

2.2.6 Optical Splitters

Originally, the system design was developed using standard multimode 62.5 μm fiber core and the corresponding 1:2 splitters were easy to obtain from a number of vendors. The push to use larger core fibers may complicate finding potential vendors capable of working with fiber of this size. Ophir is currently working on another Research & Development project that requires similar large core fiber splitters that will transmit in the ultraviolet wavelength region. Ophir has located a vendor that will build these splitters and soon, Ophir will submit a set of revised specifications to this vendor reflecting the need for large fiber that transmits in the near-IR region.

2.2.7 System Software Design

The data acquisition and display software for the airborne application has been completed. Most of the data algorithms for retrieving gas concentration data from the raw collected data were based upon earlier software development for the ground based gas radiometry system. The user's interface is all new and is shown in Figure 22.

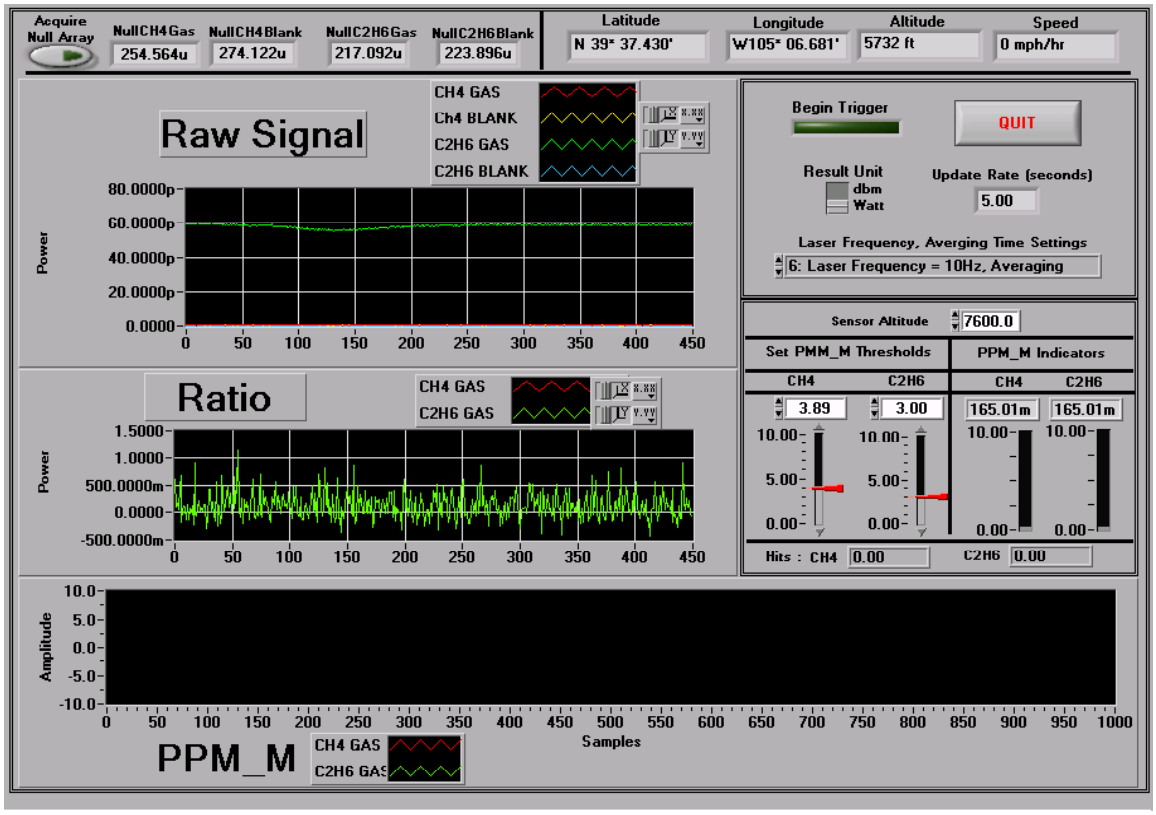

Figure 22. User's Software Interface for the Airborne Optical, Remote Sensor

The display contains information on the raw detector data, after it has been processed to separate methane and ethane data from the multiplexed data buffers. The display also shows the ratio of the retrieved gas cell over blank cell data, normalized to subtract out all common mode signals. Finally, the gas concentration data is displayed in ppm * m over the intended flight path. The Global Positioning System (GPS) data is gathered and displayed at a 1 Hz data rate. A separate display can be toggled on that will display the actual GPS route against the programmed route, identifying any deviations. High amounts of methane and ethane concentration will be automatically displayed and stored into a data file. The user can dynamically change the thresholds for the high concentration "hits" during the flight test. This data file can be accessed at any time during the flight to allow the pilot to initiate repeat passes over suspected natural gas leaks.

Ophir is currently waiting on the fiber amplifier vendor to supply interface requirements to allow the user to control the modulation rate, power output, and input trigger for the

fiber amplifier. Ophir will also be able to monitor health and status of the fiber amplifier using the standard RS-232 communication interface.

3 Project Issues

3.1 Lead-Time for Developing and Procuring the Fiber Amplifier

Ophir is receiving monthly update reports from the fiber amplifier vendor. The progress appears to be roughly on track with their original proposal to deliver the amplifier sometime in the middle to the end of June (the scheduled delivery has moved out by about a week from the original schedule). The high-risk areas for the delivery of the amplifier are related to the delivery of the high power pump amplifier and L-Band isolators capable of handling high power. The laboratory prototype is scheduled to be assembled and to begin testing the first week of May. The custom highly, non-linear fiber will be ordered once the zero non-dispersion wavelength is measured from the laboratory prototype testing.

Depending upon the contents of the next April summary report, Ophir may decide to visit the vendor's development facility to address data gathered to date, any action items such as delayed sub-system hardware deliveries, output source linewidth and spectral shape, and schedule delays.

3.2 Incorporation of Large Core Fiber Into the Airborne Transceiver

The transmitter and receiver optics for the transceiver will be connected entirely by fiber optics. This technique will add ruggedness and ease of alignment to the system. The target reflectance measurements have indicated that the size of the fiber core is critical to the amount of light seen by the detector, and the larger the core the higher the signal to the detector. It appears that the choice of 1000 μm fiber core is the largest feasible solution. This fiber is readily available and can accommodate a variety of connector styles. The numerical aperture increases as the fiber core size increases and this can make it more difficult to transmit the light down through the other system components such as the splitters, gas cells, optical filters, and detectors. Once the fiber core size and numerical aperture have been selected, Ophir will begin to locate vendors capable of interfacing to the large core. Hopefully, Ophir will be able to stay with the vendors who are presently on contract to supply us the optical fiber coupled components. Ophir has already put these vendors on hold, pending the new fiber selection and has initiated a work around request.

3.3 Advisory Panel Support for the Field Testing of Remote Sensor Leak Detection Systems at the Rocky Mountain Oilfield Test Center (RMOTC) in Casper, Wyoming

Ophir has been working with the DOE as a participant in an Advisory Panel for the testing of various competing remote sensor technologies at the RMOTC. The first

meeting was held in Casper, Wyoming on March 29th and 30th. The participating companies appeared to be quite eager and willing to help in the development of the test strategy. Ophir is excited about the opportunity to showcase it's technology in remotely detecting natural gas leaks. It looks like it will take a great deal of work to implement a comprehensive test plan that will include everyone's concerns. A two-week test window was tentatively scheduled for September 5 – 18. The next Advisory Panel meeting is set for June 8th and 9th.

4 Conclusions

Highlights of the work for this performance period include the following:

- Methane gas absorption measurements over a 10 m optical path were taken using a very narrowband low power source. The gas correlation software was not able to discern any levels of methane absorption. Next, gas correlation modeling of this setup was performed to identify the source of the problem. The narrowband source linewidth and spectral shape were input into the model, and the results were identical to those obtained in the laboratory; no absorption was seen.
- Additional modeling was done using different linewidths and spectral shapes, and a non-gaussian spectral shape with broader linewidths allowed for good discrimination of various methane concentrations down to several parts-per-million.
- The design specifications for the light source were redefined and submitted to the light source vendor. The vendor responded favorably to the changes, and indicated that the new target specifications could be incorporated into the design. The light source Purchase Order was finalized and the contract was signed in January 2004 with a five-month delivery time.
- Ophir purchased and received a large aperture telescope, which will function as the receiver portion of the co-aligned transceiver.
- Ophir conducted extensive testing of the co-aligned transceiver over a one-way optical path of 150 m (500 ft) against a Lambertian reflector. It was determined that standard multimode 62.5 μm fiber core too small to capture sufficient amounts of reflected signal. Larger core sizes up to 1000 μm proved much more useful in this regards as nearly 200 nW of return power was seen, when using the 1000 μm fiber. This power return was approximately 10 times the required value based upon signal-to-noise modeling.

Ophir has continued to eliminate the design risk to the airborne system by performing as much laboratory and field-testing as possible, prior to final system assembly. The realization that very narrowband, gaussian waveforms do not work well with the Ophir gas correlation software eliminated a significant potential problem and kept intact the goal of eliminating common mode noise through the correlation software. Potential design problems with the gas cells and narrowband fiber optic coupled filters have also been found in time to allow for larger fiber coupling, thus saving cost and time to the project.

5 References

Philip C. D. Hobbs “Building Electro-Optical Systems – Making It All Work”, John Wiley & Sons, Inc., 2000